Adrenomedullin antagonist suppresses tumor formation in renal cell carcinoma through inhibitory effects on tumor endothelial cells and endothelial progenitor mobilization

KUNIHIKO TSUCHIYA[1,2,3,4*], KYOKO HIDA[2*], YASUHIRO HIDA[5], CHIKARA MURAKI[2,3],
NORITAKA OHGA[2,3], TOMOSHIGE AKINO[2,3,4], TAKESHI KONDO[4], TETSUYA MISEKI[1],
KOJI NAKAGAWA[1], MASANOBU SHINDOH[3], TORU HARABAYASHI[4],
NOBUO SHINOHARA[4], KATSUYA NONOMURA[4] and MASANOBU KOBAYASHI[1,7]

[1]Division of Cancer Biology, Institute for Genetic Medicine, Hokkaido University; [2]Division of Vascular Biology,
[3]Division of Oral Pathobiology, Hokkaido University, Graduate School of Dental Medicine; [4]Department of Urology,
[5]Department of Surgical Oncology, [6]Department of Gastroenterology and Hematology, Hokkaido University, Graduate
School of Medicine; [7]School of Nursing & Social Services, Health Sciences University of Hokkaido, Sapporo, Japan

Abstract. Adrenomedullin (AM) is a multifunctional 52-amino acid peptide. AM has several effects and acts as a growth factor in several types of cancer cells. Our previous study revealed that an AM antagonist (AMA) suppressed the growth of pancreatic tumors in mice, although its mechanism was not elucidated. In this study, we constructed an AMA expression vector and used it to treat renal cell carcinoma (RCC) in mice. This AMA expression vector significantly reduced tumor growth in mice. In addition, microvessel density was decreased in AMA-treated tumors. To analyze the effect of AMA on tumor angiogenesis in this model, tumor endothelial cells (TECs) were isolated from RCC xenografts. TEC proliferation was stimulated by AM and it was inhibited by AMA significantly. AM induced migration of TECs and it was also blocked by AMA. However, normal ECs (NECs) were not affected by either AM or AMA. These results demonstrate that AMA has inhibitory effects on TECs specifically, not on NEC, thereby inhibiting tumor angiogenesis. Furthermore, we showed that vascular endothelial growth factor-induced mobilization of endothelial progenitor cell (EPC) into circulation was inhibited by AMA. These results suggest that AMA can be considered a good anti-angiogenic reagent that selectively targets TECs and EPC in renal cancer.

Correspondence to: Dr Kyoko Hida, Department of Oral Pathology and Biology, Division of Vascular Biology, Hokkaido University, Graduate School of Dental Medicine, N13 W7, Kita-ku, Sapporo 060-8586, Japan
E-mail: khida@den.hokudai.ac.jp

*Contributed equally

Introduction

Renal cell carcinoma (RCC) is a refractory cancer, and cytotoxic chemotherapy and radiation therapy lack effectiveness in its treatment. Until recently, the only effective treatment was cytokine therapy with interferon-α (IFN-α) or interleukin-2 (IL-2). However, only a limited subset of patients with metastatic RCC would gain clinical benefit from standard IFN-α or IL-2 therapy. Advances in understanding the underlying molecular biology of RCC have established tumor angiogenesis as a relevant therapeutic target in clear cell RCC (1,2). Approximately 60% of clear cell RCC tumors have an inactivated von Hippel-Lindau (VHL) tumor suppressor gene (3). Under normal conditions, VHL encodes a protein (referred to as pVHL) that targets hypoxia-inducible factor-1α (HIF-1α) for proteolysis. As a result of VHL gene inactivation, HIF-1α is not subject to proteolysis and inactivation. Activated HIF then translocates into the nucleus and this leads to the transcription of a variety of genes that play a central role in tumor progression. HIF-1-inducible genes include angiogenic factors such as vascular endothelial growth factor (VEGF), platelet-derived growth factor, basic fibroblast growth factor, and adrenomedullin (AM) (4,5). Among these angiogenic factors, we have been examining the role of AM in tumor formation by pancreatic cancer cells, and found that the increase in the AM mRNA level under hypoxia was markedly greater than that in the VEGF mRNA level in accordance with a previous report (6). We demonstrated that the intratumoral injection of an adrenomedullin antagonist (AMA) inhibited tumor growth in a pancreatic cancer cell line in a xenograft mouse model (7). In addition, we recently demon-

strated that naked DNA-encoding AMA suppressed the growth of pancreatic cancer and breast cancer cell lines through the inhibition of AM (8), a multifunctional polypeptide that was originally isolated from human pheochromocytoma and is a member of the family of peptides that includes calcitonin (CT), α- and ß-calcitonin gene-related peptide (9). AM gene knockout mice have shown embryonic lethality with severe abnormalities of the vasculature (10) and subcutaneous hemorrhage indicating the significance of AM signaling in vascular development. AM is expressed in a variety of malignant tumor tissues (11,12) and was shown to be mitogenic for human cancer cell lines, including lung, breast, colon, prostate and pancreatic lineages *in vitro* (12,13). In addition, AM is considered to be angiogenic in tumors. In xenografted tumor models using human endometrial or breast tumor cell lines, vascular density or directed growth of blood vessels was increased in AM-overexpressing transfectants (14,15). Iimuro *et al* recently showed that continuous infusion of AMA peptides suppressed the growth of sarcoma and reduced the number of capillaries in mice (16). These findings suggest that AM plays an important role in tumor formation in a variety of cancers through the direct suppression of tumor cells and suppression of angiogenesis. However, there are few reports demonstrating the involvement of AM in tumor formation in RCC.

In this study, we examined the potential effects of gene therapy with naked DNA-expressing AMA on the growth of an RCC xenografted into nude mice in order to explore the role of AM in tumor formation in RCC. In order to address the mechanism of how AMA modulates angiogenesis in RCC, we isolated tumor endothelial cells (TECs) from tumor tissues and normal endothelial cells (NECs) from the dermis for comparative analysis. Furthermore, we analyzed the effects of AMA on EPC mobilization into circulation.

Materials and methods

Reagents and antibodies. The following reagents and antibodies were purchased: AM and AMA (AM22-52) (Peptide Institute Inc., Osaka, Japan); rat anti-mouse CD31 antibody (eBioscience, San Diego, CA); rat anti-mouse CD105 antibody (BD Biosciences, San Jose, CA), rat anti-mouse CD144 antibody (BD Biosciences), rat anti-mouse PE-CD54 antibody (Biolegend, San Diego, CA) Alexa Fluor 488 goat anti-rat antibody (Molecular Probes, Eugene, OR); FITC-Bandeirea Simplicifolia Lectin 1-B4 (BS1-B4; Vector Laboratories, Burlingame, CA); and 4',6-diamidino-2-phenylindole (DAPI; Roche, Indianapolis, IN).

Cells and cell culture. The OS-RC-2 human RCC cell line was purchased from Riken Cell Bank (Tsukuba, Japan). These cells were cultured in a humidified atmosphere of 5% CO_2 and 95% air at 37˚C in RPMI-1640 medium (Sigma, St. Louis, MO) supplemented with 10% heat-inactivated fetal bovine serum (FBS).

The A375SM super-metastatic human malignant melanoma cell line was kindly gifted by Dr I.J. Fidler (M.D. Anderson Cancer Center, Houston, TX). The cells were cultured under the same conditions in minimum essential medium (MEM; Gibco, Grand Island, NY) supplemented

with 10% heat-inactivated FBS. The medium was changed every 3 days.

Animals and treatments. Pathogen-free, 6-week-old female nude mice (nu/nu) weighing ~20 g, were obtained from Sankyo Labo Service Corporation (Tokyo, Japan) and were randomly divided into two groups (n=6 in each group). Tumor cells (OS-RC-2; $5x10^6$ cells/mouse) were inoculated subcutaneously into the right flank of the mice. After tumor induction (day 0), naked DNA-encoding AMA was injected intramuscularly using the ultrasound-microbubble method as described previously (8) when the tumor size reached an average diameter of 4 mm (on day 13). The shortest and longest diameters of the tumor were measured on the treatment day, and tumor volume (mm^3) was calculated using the following standard formula: (shortest diameter)^2 x (longest diameter) x 0.5. There were no differences in body weight among the groups throughout the experiment. Mice were sacrificed under anesthesia on day 21. All procedures for animal experimentation were approved by the local animal research authority and animal care was in accordance with institutional guidelines.

Immunohistochemical analysis and determination of microvessel density (MVD). Tumors were dissected from mice after the mice were sacrificed and divided along the longest diameter using a surgical knife. The specimens were embedded in cryocompound (Tissue-Tek; Miles, Elkhart, IN) and immediately immersed in liquid nitrogen. The frozen specimens were sectioned to obtain 10-μm thick sections using a cryotome. Frozen sections were fixed in 100% ice-cold acetone for 10 min and blocked with 2% goat and 5% sheep serum in PBS for 30 min. Sections were incubated with rat anti-mouse CD31 antibody for 16 h followed by Alexa Fluor 488 goat anti-rat antibody for 2 h. Sections were counterstained with DAPI. Images were obtained randomly using an Olympus IX-71 microscope (Olympus, Tokyo, Japan). To analyze MVD, the number of vessels per unit area in CD31-stained sections was determined using the MetaMorph software (Molecular Devices, Tokyo, Japan).

Isolation of TECs. ECs were isolated with modifications as described previously (17). Briefly, TECs were isolated from RCC (OS-RC-2) and melanoma (A375SM) xenografts in nude mice. NECs were isolated from dermis as control. ECs were isolated using a magnetic cell-sorting system (Miltenyi Biotec, Bergisch Gladbach, Germany) according to the manufacturer's instructions using FITC-anti-CD31 antibody. CD31-positive cells were sorted and plated onto 1.5% gelatin-coated culture plates and grown in EGM-2 MV (Clonetics, Walkersville, MD) and 15% FBS. Diphtheria toxin (500 ng/ml; Calbiochem, San Diego, CA) was added to the TEC cultures to kill any remaining human tumor cells (18) and also to TECs, so that all ECs were treated in the same manner. The isolated ECs were subjected to a second round of purification using FITC-BS1-B4 and their purity was determined as described previously (17).

Cell proliferation. Cell proliferation was measured with the MTS assay. Cultured cells were seeded at $2x10^3$ cells per well
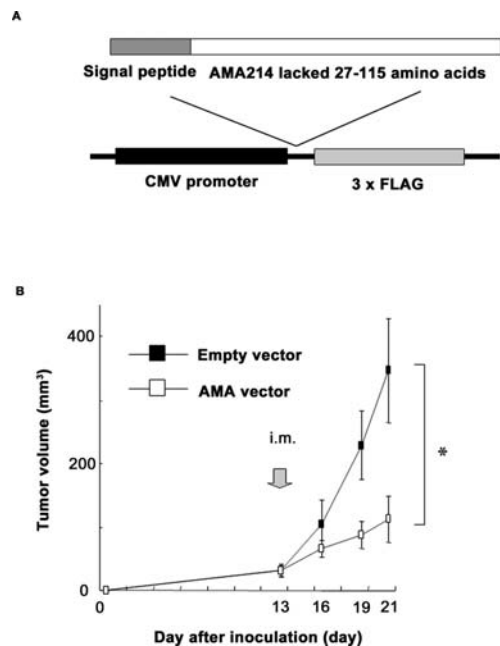
Figure 1. Effects of gene therapy with AM antagonist; AM (22-52), AMA. (A) An AMA expression vector (p3*FLAG-CMV14) was constructed. (B) OS-RC-2 cells (renal cancer cell line) were inoculated subcutaneously into nude mice. Tumors were treated on day 13 by intramuscular injection of the AMA expression vector. The AMA expression vector significantly reduces tumor growth in mice compared with the control vector. *P<0.01, versus control. Points represent the mean (n=6) and bars show the SD.

in 96-well flat-bottomed plates in a suitable medium (RPMI-1640 or MEM for tumor cells and EGM-2 MV for ECs) and allowed to adhere for 12 h. After 24 h of starvation (serum- and growth factor-free medium; EBM-2), AM (10^{-6} mol/l) or AM (10^{-6} mol/l) + AMA (10^{-5} mol/l) was added. After 72 h, the proliferative activity was determined by the MTS assay (CellTiter-96 non-radioactive cell proliferation assay; Promega, Madison, WI), which monitors the number of viable cells, according to the manufacturer's instructions. The results represent the average of 6 wells per cell line. The experiment was carried out three times with similar results.

Cell migration. Cell migration was measured in a Boyden chamber as described previously with modifications (19). Cells were starved in EBM-2 medium for 24 h and then pretreated with AM (10^{-7} mol/l) or AM (10^{-7} mol/l) + AMA (10^{-7} mol/l) for 24 h. Pretreated ECs (1×10^4) in EBM-2/0.5% FBS were seeded in the upper chambers and EBM-2 containing 10 ng/ml VEGF was added in the lower chambers as a chemoattractant. After 4 h at 37°C, cells that migrated through a fibronectin (5 μg/ml)-coated polycarbonate membrane (8-μm pores; Corning Costar, Nagog Park, MA) were fixed in 2% paraformaldehyde and stained with DAPI. The number of cells that migrated to the lower side of the filter was counted after the cells on the upper side were wiped off the membrane. The data are presented as the average of three counts ± SD. The experiment was carried out three times with similar results.

Reverse transcription-PCR (RT-PCR) and quantitative real-time RT-PCR. RT-PCR: RNA was isolated using the RNeasy micro kit (Qiagen, Valencia, CA) using RNase-free DNAse

set (Qiagen) according to the manufacturer's instructions. Total RNA was then reverse-transcribed using M-MLV reverse transcriptase (Invitrogen, Carlsbad, CA). The cDNA product was amplified with specific primers. The primers were as follows: CRLR forward, 5'-GCAGGGACGGAATCAATGCAGT-3'; reverse, 5'-GGTAGAACAGATTCAGGGCTG-3'. RAMP2 forward, 5'-CTGAGGACAGCCTTGTGTCA-3'; reverse, 5'-TTCTGCAGGTCGCTGTAATG-3'. RAMP3 forward, 5'-GAAGACCCCAGCACAGCGGCT-3'; reverse, 5'-GCCACCTTCTGCATCATGTCA-3'. GAPDH forward, 5'-TCTGACGTGCCGCCTGGAG-3'; reverse, 5'-TCGCAGGAGACAACCTGGTC-3'.

The thermal cycle profile consisted of an initial denaturation step at 95°C for 3 min followed by 35 cycles consisting of denaturation for 20 sec at 95°C, annealing of primers for 20 sec at 57°C, followed by a final 15 sec extension at 72°C. Amplified PCR products were separated on 2% agarose gels and visualized with ethidium bromide. GAPDH was used as a loading control.

Quantitative real-time PCR: RNA (5 μg) was used in a 15-μl reaction volume and PCR was conducted using the DyNAmo SYBR-Green qPCR Kit (Finnzymes, Espoo, Finland) according to the manufacturer's instructions. Cycling conditions were according to the manufacturer's instructions based on the use of Opticon Monitor version 3.0 (Bio-Rad, Hercules, CA). Briefly, cycling comprised polymerase activation for 15 min at 95°C followed by PCR; then, 40 cycles of 15 sec at 95°C, 15 sec at 57°C, and 20 sec at 72°C. Expression levels were normalized to those of GAPDH.

Counting the number of CD133+/VEGFR2+ cells to estimate the number of EPCs. PBS or VEGF (300 ng) was injected intraperitoneally into 10 nude mice in each group to mobilize EPCs from the bone marrow as described previously (20). In each group, AM (0.5 mg/kg), AM (0.5 mg/kg) + AMA (0.5 mg/kg), or vehicle was injected once a day for 2 days. Injection of AM or AMA into nude mice had no toxic effects. Forty-eight hours after the first injection, peripheral blood (700-1000 μl) was collected under anesthesia from each mouse in each group (n=5 for each group) before they were sacrificed. Mononuclear cells were isolated by sucrose gradient centrifugation from peripheral blood with modifications as described previously (21), and the number of cells was counted. Next, the cells were incubated with FITC-conjugated anti-mouse CD133 and PE-conjugated anti-mouse VEGFR2 in order to count the number of CD133+/VEGFR2+ cells by flow cytometry. Flow cytometry was performed using a FACSCalibur flow cytometer (BD Biosciences) with analysis gates. A minimum of 10,000 events were counted for each mouse.

Statistical analysis. Differences between the groups were statistically evaluated using Student's t-test. Results are presented as mean ± SD. The P-values were two-tailed, and P<0.01 was considered statistically significant.

Results

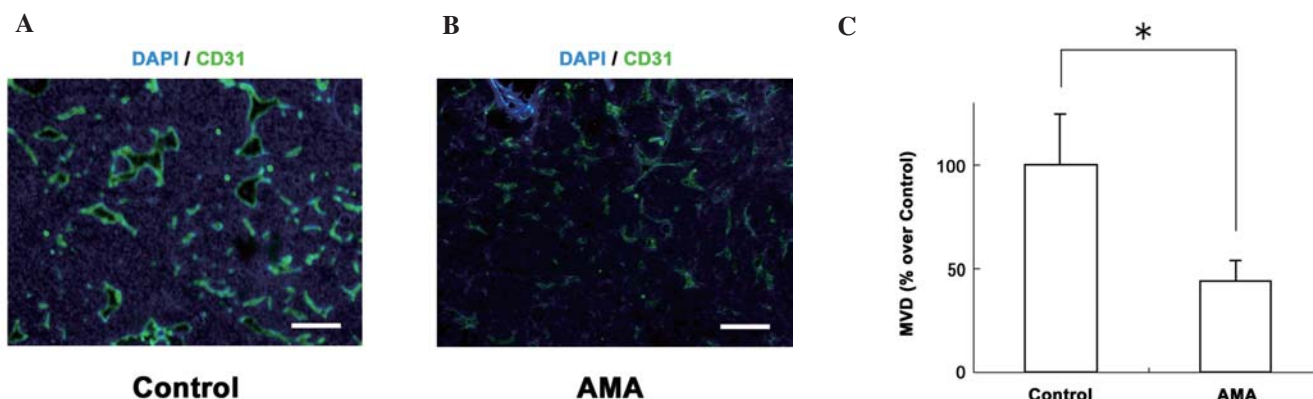*Naked DNA-encoding AMA suppresses tumor growth*. The naked DNA-encoding AMA (AMA vector) (Fig. 1A) was

Figure 2. Microvessel density (MVD) is significantly decreased in tumors treated with the AMA expression vector. (A) Snap-frozen tumor tissue specimens were processed for immunohistochemistry after the mice were sacrificed. Cryosections were stained with FITC-labeled anti-CD31 antibody and counterstained with DAPI. Representative images of the control vector (A) and AMA expression vector-treated tumors (B) are shown. The CD31-positive vessel area is decreased in AMA expression vector-treated tumor compared with control tumors. Bars in A and B, 100 µm. (C) Quantitative analysis of MVD comparing the AMA expression vector-treated group with the control group. MVD is significantly lower in AMA expression vector-treated tumors than in control tumors. *P<0.01 versus control (n=6).
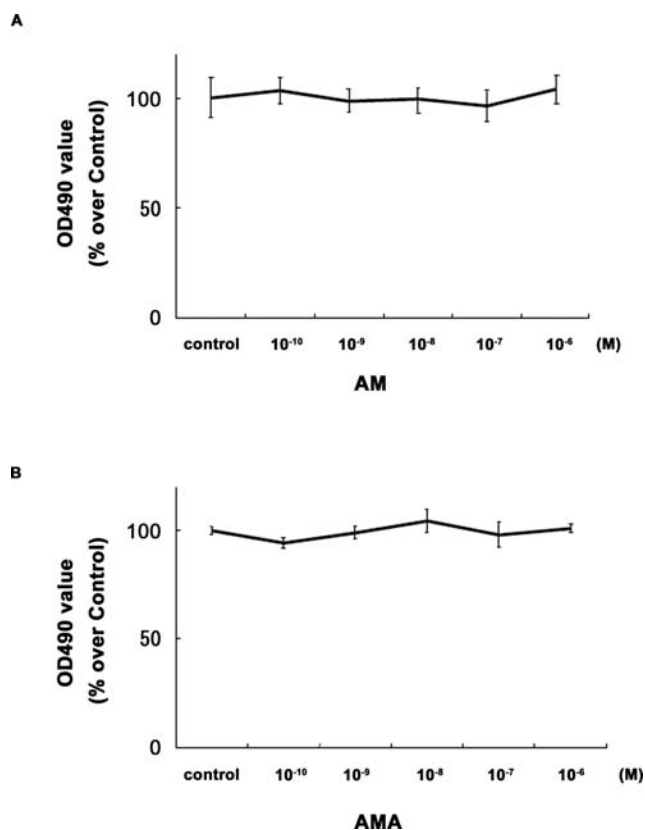

Figure 3. Assay for OS-RC-2 renal cancer cell proliferation *in vitro*. The cells were serum-starved for 24 h and incubated with AM or AMA for 72 h. Cell number was estimated by the MTS assay. (A) AM did not affect proliferation in the range 10^{-10}-10^{-6} mol/l. (B) AMA did not affect proliferation in the range 10^{-10}-10^{-6} mol/l.

injected intramuscularly using the ultrasound-microbubble method when the tumor size reached an average diameter of 4 mm (on day 13), as described previously (8). The growth of tumors treated with AMA vector was significantly suppressed compared with that of tumors treated with an empty vector (mean ± SD tumor volume on day 21, 112.7±36.3 mm³

vs. 346.6±81.9 mm³; P<0.01) (Fig. 1B). Treatment with the vectors was well-tolerated without apparent toxicity or changes in body weight throughout the study.

AMA inhibits tumor angiogenesis. Snap-frozen tissue specimens were processed for immunohistochemical study when the mice were sacrificed. Cryosections were stained with anti-CD31 antibody and digital images were obtained. Morphometric analysis was performed on digital images from each group using MetaMorph software. The CD31-stained area (MVD) was measured in each group treated with AMA vector or control vector. The MVD of the tumors treated with AMA vector was only half of that of the tumors treated with control vector (Fig. 2A and B) and the difference was significant (P<0.01) (Fig. 2C). Tumors treated with AMA vector contained large necrotic lesions, possibly as a result of insufficient blood supply.

Neither AM nor AMA affects in vitro proliferation of OS-RC-2 cells. We investigated whether AM or AMA affected the proliferation of OS-RC-2 renal carcinoma cells *in vitro* using the MTS assay. OS-RC-2 cells did not respond to AM (10^{-10} mol/l) nor AMA (10^{-6} mol/l) (Fig. 3A and B). Therefore, it is possible that the suppression of *in vivo* tumor growth was not due to the inhibitory effect of AMA on cell proliferation of OSRC-2 cells.

Proliferation of TECs is stimulated by AM. AM promoted tumor growth through the stimulation of angiogenesis in tumor tissues and AMA significantly reduced tumor vasculature in our previous studies using a mouse tumor model (7). To address the mechanism of how AMA modulates the endothelium in tumors, we next isolated TECs (renal carcinoma ECs) from RCC xenografts in nude mice and NECs (skin ECs) from mouse dermis for comparative analysis. In addition, we used the TEC (melanoma EC) isolated from melanoma as well, which have been used in our previous studies. All ECs were isolated and maintained under similar conditions as described previously (17), and ECs were characterized by
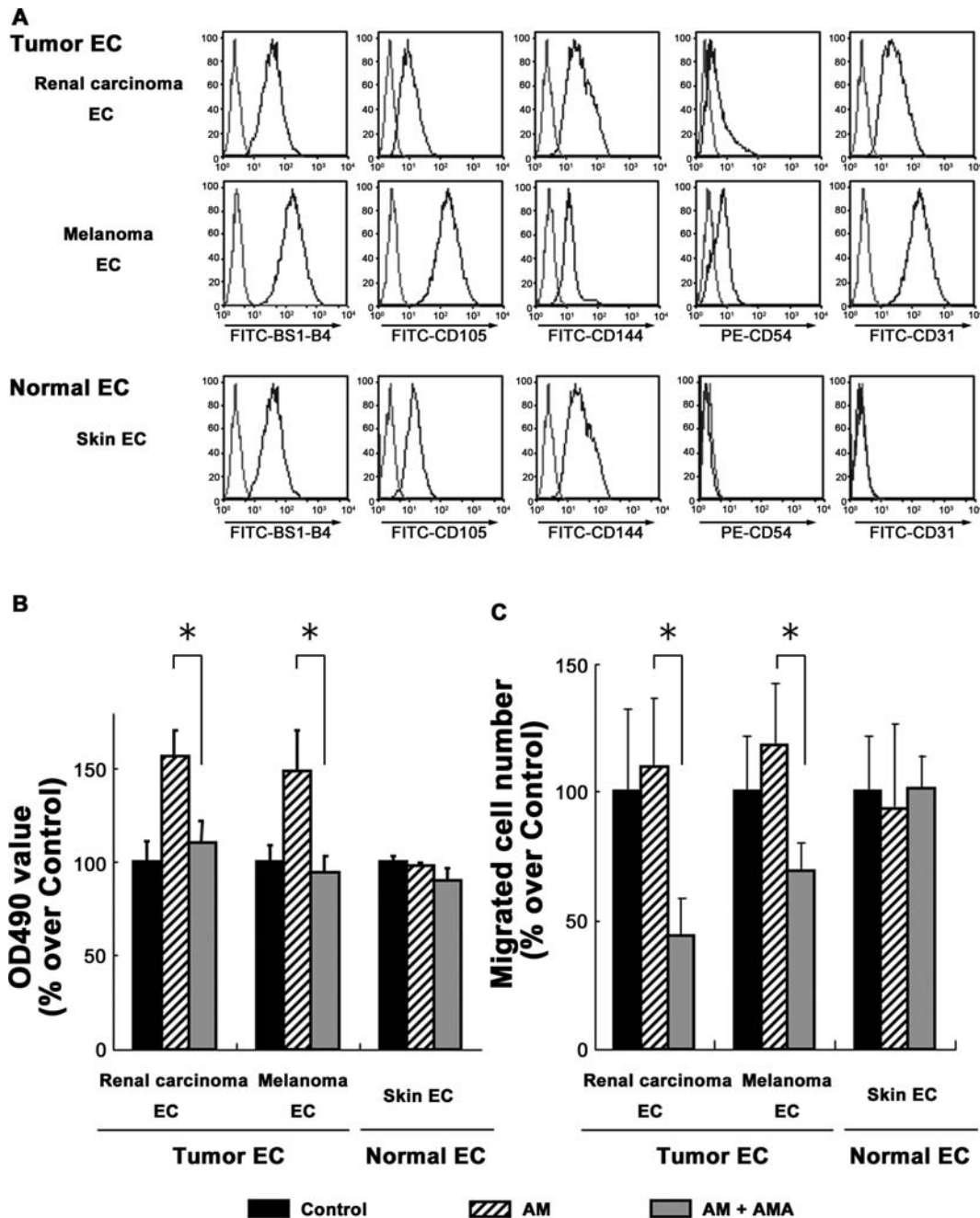
Figure 4. AMA-suppressed cell proliferation and migration of TECs. (A) Isolation and characterization of tumor and normal ECs. TECs were isolated from human carcioma (renal cancer, melanoma) xenografts and NECs counterparts were obtained from dermis of nude mice as described previously. Flow cytometry of TECs binding to FITC-BS1-B4, CD105, CD144, CD54 and CD31 to analyze EC marker expression. Lighter lines are EC-positive for these marker and bold lines show control. Both TECs show the EC marker expression. (B) Proliferation of ECs *in vitro*. The cells were serum-starved for 24 h and incubated with AM or AMA for 72 h. The number of cells was estimated by the MTS assay. AM (10^{-6} mol/l) promotes the proliferation of TECs but not that of normal ECs. AMA (10^{-5} mol/l) blocks AM-induced proliferation of tumor ECs. *P<0.01 versus control (n=5). (C) Migration of ECs *in vitro*. The cells were pretreated (AM 10^{-7} mol/l, AM 10^{-7} mol/l + AMA 10^{-7} mol/l) for 24 h and seeded into the upper chambers. VEGF (10 ng/ml) was added to the lower chambers. AM-induced migration of TECs is inhibited by AMA. *P<0.01 versus control.

FACS analysis with FITC-BS-B4, which binds to mouse endothelial cells, CD105, CD144, CD54, CD31 to see endothelial cell marker expression (Fig. 4A). Both TECs showed the EC marker expression and NECs expressed most of them with downregulation of CD54 and CD31. The purity of each EC line was greater than 96% addressed by BS1-B4 binding. Then, we examined the effect of AM and AMA on the growth of these EC lines. AM stimulated the proliferation of renal ECs and melanoma ECs, but not skin ECs. Addition of

AMA abrogated the stimulatory effect of AM on the growth of renal ECs and melanoma ECs, as measured by the MTS assay (Fig. 4B).

AMA inhibits VEGF-induced TEC migration. AMA is reported to inhibit migration of normal ECs such as human umbilical vein ECs (HUVECs) *in vitro* (22). However, the effects of migration on TECs remain to be elucidated. In this study, we examined VEGF-stimulated migration of ECs after
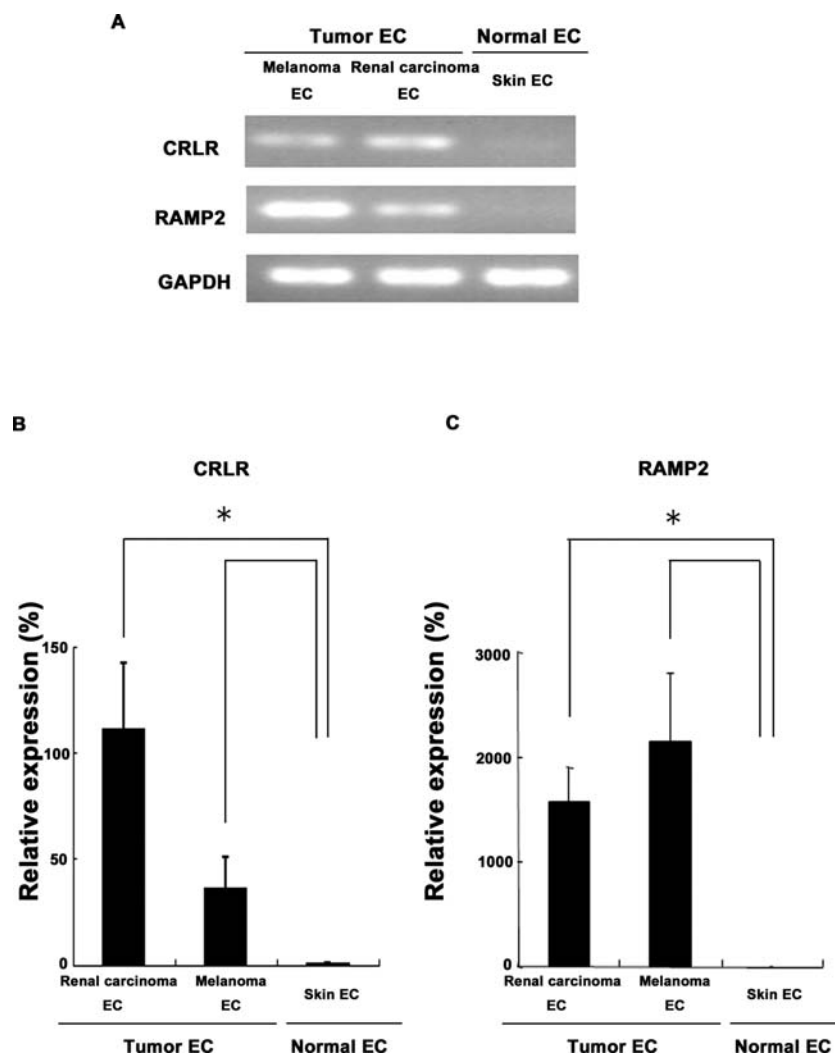
Figure 5. ECs were analyzed by PCR for AM receptors. (A) Total RNA from all ECs was extracted and assessed for the expression of CRLR and RAMP2 mRNAs by reverse transcription followed by PCR with oligonucleotide primers. PCR products detected on ethidium bromide-stained gels are 172- and 128-bp fragments generated from mRNAs of CRLR, and RAMP2 respectively. (B and C) We also analyzed the pattern of AM receptor expression by real-time PCR using SYBR-Green. *P<0.01, versus controls.

treatment with AM (10^{-7} mol/l) or AMA (10^{-7} mol/l), which was measured as the number of cells migrating through a fibronectin-coated membrane within 4 h, using a Boyden chamber. AMA significantly inhibited VEGF (10 ng/ml)-induced TEC migration (P<0.01) (Fig. 4C). The number of AMA-treated TECs that migrated was only half the number of untreated TECs that migrated. On the other hand, the migration of NECs was not affected by AMA in the same experimental conditions as those used for TECs. These results demonstrate that AMA has specific inhibitory effects on TECs, but not on NECs, thereby causing the inhibition of tumor angiogenesis.

The expression pattern of AM receptors differs between TECs and NECs. The action of AM is specific and is mediated by calcitonin receptor-like receptor/receptor activity-modifying protein-2 and -3 (CRLR/RAMP2; CRLR/RAMP3) receptors (9). Total RNA from all ECs was extracted and analyzed for the expression of CRLR, RAMP2 and RAMP3 mRNAs using reverse transcription followed by PCR with specific oligonucleotide primers. The sizes of PCR products for CRLR, RAMP2 and RAMP3 were 172, 128 and 129 bp,

respectively. CRLR was clearly detected in both melanoma ECs and OS-RC-2 ECs, but only very faintly in skin ECs. RAMP2 was clearly detected in tumor ECs but only very faintly in skin ECs (Fig. 5A). RAMP3 was detected in melanoma ECs and skin ECs, but not in renal ECs (data not shown). We also analyzed AM receptor expression levels by real-time PCR. Both tumor ECs, but not skin ECs expressed CRLR and RAMP2 mRNA. The expression levels of CRLR mRNA in melanoma ECs and renal ECs was 30- and 100-fold higher, respectively, than that in skin ECs (Fig. 5B). In particular, the expression level of RAMP2 by TECs was significantly higher than that by NECs (P<0.01) (Fig. 5C). The expression levels of RAMP2 mRNA in melanoma ECs, and renal ECs was 1500- and 2000-fold higher, respectively, than that in skin ECs (Fig. 5C). These data suggest that the higher expression levels of RAMP2 and CRLR may lead to a higher response of TECs to AM and AMA compared with NECs.

AMA suppresses VEGF-stimulated mobilization of CD133+/ VEGFR2+ cells into circulation. To evaluate the effect of AMA on EPC mobilization, the number of CD133+/VEGFR2+ cells

EPC mobilization
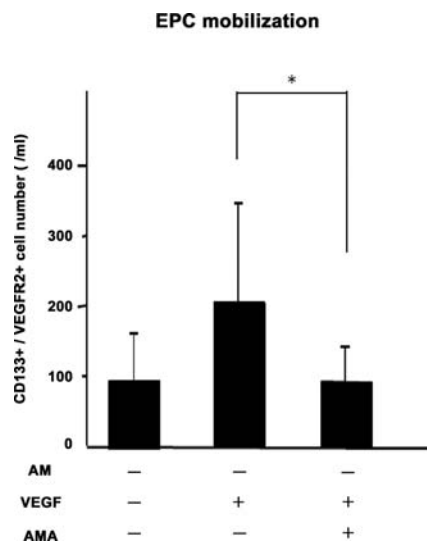

Figure 6. AMA suppresses VEGF-stimulated mobilization of CD133+/ VEGFR2+ cells into circulation. Ten nude mice in each group were injected intraperitoneally with PBS or a high dose of VEGF (300 ng) to mobilize EPCs from the bone marrow. Next, in each group, EGCG (5 mg/kg) or vehicle was injected once a day for 2 days. Forty-eight hours later, peripheral blood was collected from each mouse in each group (n=10 for each group) before they were sacrificed. PBMCs were collected and incubated with FITC-anti-mouse CD133 and PE–anti-mouse VEGFR2, and the number of CD133+/ VEGFR2+ cells is counted using FACS. Although there is no significant difference between the VEGF and VEGF + AMA groups, the low dose of AMA (0.5 mg/kg) significantly decreased the number of VEGF-mobilized CD133+/VEGFR2+ cells that migrate into peripheral circulation.

in circulation was analyzed in mice with or without AMA treatment. VEGF (300 ng) was injected intraperitoneally into mice to mobilize EPCs and then a low dose of AMA (0.5 mg/ kg) or vehicle (PBS) was injected once a day for 2 days. Forty-eight hours after the first injection, peripheral blood was collected from each mouse, and PBMCs were isolated and counted. PBMCs were incubated with anti-CD133 and anti-VEGF2 antibodies, and the CD133+/VEGFR2+ cells in circulation were counted using FACS. AMA alone did not affect the number of CD133+/VEGFR2+ cells. However, in VEGF-treated mice, the number of circulating CD133+/ VEGFR2+ cells was low after treatment with a low dose of AMA (Fig. 6). These results suggest that AMA inhibits the VEGF-induced mobilization of EPCs into circulation.

Discussion

In this study, we clearly demonstrated that naked DNA-encoding AMA significantly inhibited the in vivo growth of RCC with inhibition of tumor angiogenesis. In addition, we showed that TECs had higher response to AM and AMA, compared with NECs. Furthermore, AMA inhibited the mobilization of endothelial progenitor cells stimulated by VEGF.

There are some reports showing that AM is essential for the growth of several cancers in vivo (12,23-25). We showed that the intratumoral injection of AMA peptides suppressed tumor formation by human pancreatic cancer cells in nude mice (7) and that intramuscular injection of naked DNA-encoding AMA almost completely suppressed tumor

formation in mammary and pancreatic cancer cells in SCID mice (8). In the present study, we showed that OS-RC-2, an RCC cell line, expressed AM both under normoxia and hypoxia (data not shown). This is consistent with previous reports that AM is overexpressed in several cancer types. Furthermore, we showed that OS-RC-2 tumor growth was suppressed by injecting an AMA expression vector, even when injected after the tumor grew to 4 mm in diameter. This is very important in terms of cancer therapy, and these results suggest that AMA could be used in the treatment of patients at late stages of cancer.

To date, two possible mechanisms by which AM supports tumor growth in vivo have been postulated. The first possibility is that AM directly promotes tumor proliferation and survival. Several AM-overexpressing human carcinoma cell lines exhibit enhanced growth in vitro and in vivo to a varying degree (15,25). A recent report demonstrated that AMA inhibited the proliferation and invasion of pancreatic cancer cells expressing AM receptors in vitro (13). However, we found that neither AM nor AMA affected the growth of OS-RC-2 renal cancer cells in vitro, even though OS-RC2 tumor sizes in mice were clearly reduced by AMA. It was suggested that the effect of AM on tumor growth may depend on tumor cell type and that AM has no effect on the growth of RCC cells.

The second possible mechanism is that AM promotes tumor growth by stimulating angiogenesis. There have been several reports suggesting that AM stimulates normal ECs such as HUVECs to proliferate. However, there are also controversial reports that the proliferation of rat ECs are not affected by AM (24). In addition, there has been no study on the direct effect of AM on TECs even though evidence is accumulating that TECs differ from NECs, for example, in terms of change in morphology, rate of cell proliferation, gene expression and drug sensitivity (26).

We have described the isolation of TECs from human tumor xenografts in nude mice (17) and showed that TECs differed from NECs in many respects. Recent findings demonstrated the enhanced responsiveness of TECs to EGF, associated with a change in the expression of EGF receptor, compared with that of NECs (27). Furthermore, TECs were found to be cytogenetically abnormal (17,28). This prompted us to hypothesize that TECs may differ from NECs in their response to AM.

To address this question, we isolated TECs from a renal tumor xenograft model in nude mice, in which we observed an antitumor effect of AMA vector, and isolated NECs from normal skin tissue as a counterpart for comparative analysis. Interestingly, TECs differed from NECs in their response to AM and AMA. Cell proliferation was more enhanced in TECs than in NECs by AM. The proliferation of TECs stimulated by AM was reduced by AMA to baseline, whereas NECs were affected neither by AM nor AMA. Furthermore, AMA inhibited VEGF-induced cell migration in TECs but not NECs. To address the mechanism of the differential response to AM between TECs and NECs, we analyzed the expression levels of AM receptors in both TECs and NECs. Comparative analysis of the expression profiles of the four AM receptor family members showed that TECs expressed CRLR and RAMP2, whereas NECs expressed neither of

these. It may be that the differential response between TECs and NECs to AM might result from the different expression levels of AM receptors.

EPCs are currently considered a novel target for anti-angiogenic therapy, as are TECs, since they play important roles in tumor metastasis (29). It has been shown that tumors mobilize bone marrow-derived EPCs, besides recruiting neighboring blood vessels or ECs, and that EPCs migrate to tumors and become incorporated into their developing vasculature (30). Several anti-angiogenic drugs have been reported to produce inhibitory effects on EPCs. EPCs are considered to express CD133 and VEGFR2 (20). In the present study, AMA inhibited the mobilization of VEGFR2⁺/CD133⁺ cells into circulation induced by VEGF. AMA may target EPCs that are incorporated into tumor vessels and hence inhibit tumor angiogenesis. These results indicate that AMA may be effective in anti-angiogenesis therapy by specifically targeting the tumor, but not normal vasculature.

Acknowledgments

References

1. Coppin C, Porzsolt F, Awa A, Kumpf J, Coldman A and Wilt T: Immunotherapy for advanced renal cell cancer. Cochrane Database Syst Rev: CD001425, 2005.
2. Fyfe GA, Fisher RI, Rosenberg SA, Sznol M, Parkinson DR and Louie AC: Long-term response data for 255 patients with metastatic renal cell carcinoma treated with high-dose recombinant interleukin-2 therapy. J Clin Oncol 14: 2410-2411, 1996.
3. Rini BI and Small EJ: Biology and clinical development of vascular endothelial growth factor-targeted therapy in renal cell carcinoma. J Clin Oncol 23: 1028-1043, 2005.
4. Turner KJ, Moore JW, Jones A, *et al*: Expression of hypoxia-inducible factors in human renal cancer: relationship to angiogenesis and to the von Hippel-Lindau gene mutation. Cancer Res 62: 2957-2961, 2002.
5. Takahashi A, Sasaki H, Kim SJ, Tobisu K, Kakizoe T, Tsukamoto T, Kumamoto Y, Sugimura T and Terada M: Markedly increased amounts of messenger RNAs for vascular endothelial growth factor and placenta growth factor in renal cell carcinoma associated with angiogenesis. Cancer Res 54: 4233-4237, 1994.
6. Fujita Y, Mimata H, Nasu N, Nomura T, Nomura Y and Nakagawa M: Involvement of adrenomedullin induced by hypoxia in angiogenesis in human renal cell carcinoma. Int J Urol 9: 285-295, 2002.
7. Ishikawa T, Chen J, Wang J, *et al*: Adrenomedullin antagonist suppresses in vivo growth of human pancreatic cancer cells in SCID mice by suppressing angiogenesis. Oncogene 22: 1238-1242, 2003.
8. Miseki T, Kawakami H, Natsuizaka M, *et al*: Suppression of tumor growth by intra-muscular transfer of naked DNA encoding adrenomedullin antagonist. Cancer Gene Ther 14: 39-44, 2007.
9. Fernandez-Sauze S, Delfino C, Mabrouk K, Dussert C, Chinot O, Martin PM, Grisoli F, Ouafik L and Boudouresque F: Effects of adrenomedullin on endothelial cells in the multistep process of angiogenesis: involvement of CRLR/RAMP2 and CRLR/RAMP3 receptors. Int J Cancer 108: 797-804, 2004.
10. Shindo T, Kurihara Y, Nishimatsu H, *et al*: Vascular abnormalities and elevated blood pressure in mice lacking adrenomedullin gene. Circulation 104: 1964-1971, 2001.
11. Hata K, Takebayashi Y, Akiba S, Fujiwaki R, Iida K, Nakayama K, Nakayama S, Fukumoto M and Miyazaki K: Expression of the adrenomedullin gene in epithelial ovarian cancer. Mol Hum Reprod 6: 867-872, 2000.
12. Rocchi P, Boudouresque F, Zamora AJ, Muracciole X, Lechevallier E, Martin PM and Ouafik L: Expression of adrenomedullin and peptide amidation activity in human prostate cancer and in human prostate cancer cell lines. Cancer Res 61: 1196-1206, 2001.
13. Ramachandran V, Arumugam T, Hwang RF, Greenson JK, Simeone DM and Logsdon CD: Adrenomedullin is expressed in pancreatic cancer and stimulates cell proliferation and invasion in an autocrine manner via the adrenomedullin receptor, ADMR. Cancer Res 67: 2666-2675, 2007.
14. Oehler MK, Fischer DC, Orlowska-Volk M, Herrle F, Kieback DG, Rees MC and Bicknell R: Tissue and plasma expression of the angiogenic peptide adrenomedullin in breast cancer. Br J Cancer 89: 1927-1933, 2003.
15. Martinez A, Vos M, Guedez L, *et al*: The effects of adrenomedullin overexpression in breast tumor cells. J Natl Cancer Inst 94: 1226-1237, 2002.
16. Iimuro S, Shindo T, Moriyama N, Amaki T, Niu P, Takeda N, Iwata H, Zhang Y, Ebihara A and Nagai R: Angiogenic effects of adrenomedullin in ischemia and tumor growth. Circ Res 95: 415-423, 2004.
17. Hida K, Hida Y, Amin DN, Flint AF, Panigrahy D, Morton CC and Klagsbrun M: Tumor-associated endothelial cells with cytogenetic abnormalities. Cancer Res 64: 8249-8255, 2004.
18. Arbiser JL, Raab G, Rohan RM, Paul S, Hirschi K, Flynn E, Price ER, Fisher DE, Cohen C and Klagsbrun M: Isolation of mouse stromal cells associated with a human tumor using differential diphtheria toxin sensitivity. Am J Pathol 155: 723-729, 1999.
19. Ohga N, Hida K, Hida Y, Muraki C, Tsuchiya K, Matsuda K, Ohiro Y, Totsuka Y and Shindoh M: Inhibitory effects of epigallocatechin-3 gallate, a polyphenol in green tea, on tumor-associated endothelial cells and endothelial progenitor cells. Can Sci (In press).
20. Asahara T, Takahashi T, Masuda H, Kalka C, Chen D, Iwaguro H, Inai Y, Silver M and Isner JM: VEGF contributes to postnatal neovascularization by mobilizing bone marrow-derived endothelial progenitor cells. EMBO J 18: 3964-3972, 1999.
21. Sharpe EE, 3rd Teleron AA, Li B, Price J, Sands MS, Alford K and Young PP: The origin and in vivo significance of murine and human culture-expanded endothelial progenitor cells. Am J Pathol 168: 1710-1721, 2006.
22. Miyashita K, Itoh H, Sawada N, Fukunaga Y, Sone M, Yamahara K, Yurugi-Kobayashi T, Park K and Nakao K: Adrenomedullin provokes endothelial Akt activation and promotes vascular regeneration both in vitro and in vivo. FEBS Lett 544: 86-92, 2003.
23. Miller MJ, Martinez A, Unsworth EJ, Thiele CJ, Moody TW, Elsasser T and Cuttitta F: Adrenomedullin expression in human tumor cell lines. Its potential role as an autocrine growth factor. J Biol Chem 271: 23345-23351, 1996.
24. Kato H, Shichiri M, Marumo F and Hirata Y: Adrenomedullin as an autocrine/paracrine apoptosis survival factor for rat endothelial cells. Endocrinology 138: 2615-2620, 1997.
25. Oehler MK, Norbury C, Hague S, Rees MC and Bicknell R: Adrenomedullin inhibits hypoxic cell death by upregulation of Bcl-2 in endometrial cancer cells: a possible promotion mechanism for tumour growth. Oncogene 20: 2937-2945, 2001.
26. Hida K, Hida Y and Shindoh M: Understanding tumor endothelial cell abnormalities to develop ideal anti-angiogenic therapies. Cancer Sci 99: 459-466, 2008.
27. Amin DN, Hida K, Bielenberg DR and Klagsbrun M: Tumor endothelial cells express epidermal growth factor receptor (EGFR) but not ErbB3 and are responsive to EGF and to EGFR kinase inhibitors. Cancer Res 66: 2173-2180, 2006.
28. Hida K and Klagsbrun M: A new perspective on tumor endothelial cells: unexpected chromosome and centrosome abnormalities. Cancer Res 65: 2507-2510, 2005.
29. Rafii S, Lyden D, Benezra R, Hattori K and Heissig B: Vascular and haematopoietic stem cells: novel targets for anti-angiogenesis therapy? Nat Rev Cancer 2: 826-835, 2002.
30. Lyden D, Hattori K, Dias S, *et al*: Impaired recruitment of bone-marrow-derived endothelial and hematopoietic precursor cells blocks tumor angiogenesis and growth. Nat Med 7: 1194-1201, 2001.